TRENDS IN SCIENCES 2026; 23(11): 13669
https://doi.org/10.48048/tis.2026.13669 RESEARCH ARTICLE

Modulation of BAX/BCL-2 Expression and Cyclophilin A-Targeted *In Silico* Study by *Spatholobus littoralis* Combined with Doxorubicin in DMBA-Induced Breast Cancer Rat Model

Ois Nurcahyanti[1,2], Kusmardi Kusmardi[3,4,5], Noorwati Sutandyo[6,7] Aryo Tedjo[8] and Vivian Soetikno[9,*]

[1]*Doctoral Program in Biomedical Science, Faculty of Medicine, Universitas Indonesia, Jakarta, Indonesia*
[2]*Department Medical Laboratory Technology, Faculty of Health Sciences and Technology, Universitas Binawan, Jakarta, Indonesia*
[3]*Department of Pathological Anatomy, Faculty of Medicine, Universitas Indonesia, Jakarta, Indonesia*
[4]*Human Cancer Research Center, IMERI, Universitas Indonesia, Jakarta, Indonesia*
[5]*Drug Development Research Center, IMERI, Jakarta, Indonesia*
[6]*Department of Hematology and Medical Oncology, Dharmais National Cancer Center Hospital, Jakarta, Indonesia*
[7]*Department of Internal Medicine, Faculty of Medicine, Universitas Indonesia, Jakarta, Indonesia*
[8]*Department of Medical Chemistry, Faculty of Medicine, Universitas Indonesia, Jakarta, Indonesia*
[9]*Department of Pharmacology and Therapeutics, Faculty of Medicine, Universitas Indonesia, Jakarta, Indonesia*

([*]Corresponding author's e-mail: vivian.soetikno@ui.ac.id)

Received: 23 February 2026, Revised: 11 April 2026, Accepted: 18 April 2026, Published: 1 June 2026

Abstract

Cyclophilin A (CypA) has been identified as a key regulator of apoptosis and contributes to chemotherapy resistance in breast cancer cells. One indicator of apoptosis imbalance is the BAX/BCL-2 ratio, where a low ratio is associated with tumor progression and reduced treatment efficacy. Overcoming this resistance remains a challenge, particularly through combination therapies. *Spatholobus littoralis*, a flavonoid-rich medicinal plant, has shown potential as an anticancer agent, but its effectiveness as an adjuvant to doxorubicin is not fully established. This study aims to evaluate the effects of *S. littoralis* extract combined with doxorubicin on apoptosis regulation, particularly the BAX/BCL-2 expression ratio, in a DMBA-induced breast cancer rat model, and to investigate the interaction of its major compound with Cyclophilin A through molecular docking analysis. Female Sprague Dawley rats were induced with DMBA to develop breast tumors and subsequently treated with *S. littoralis* extract, doxorubicin, or their combination. Gene expression levels of BAX and BCL-2 were quantified using real-time PCR, and tumor volume and BW were monitored weekly. Data were analyzed using one-way ANOVA with post hoc tests ($p < 0.05$). Molecular docking evaluated the interaction between N-2-[4-(3,3-dimethylallyloxy)phenyl]ethylcinnamide, the plant's main compound, and CypA (PDB ID: 3RDD), while SwissADME assessed drug-likeness and pharmacokinetics. Results showed that DMBA increased BCL-2 and decreased BAX, indicating apoptosis resistance. Treatment with *S. littoralis* extract combine with doxorubicin individually significantly improved the BAX/BCL-2 ratio, reduced tumor volume, and increased %TGI, with the combination therapy producing the most pronounced pro-apoptotic effect ($p < 0.05$) and maintaining BW. Molecular docking revealed strong binding affinity of the compound to CypA, and *in silico* analysis suggested favorable drug-like properties. In conclusion, the combination of *S. littoralis* extract with doxorubicin enhances breast cancer treatment efficacy by modulating apoptosis markers, reducing tumor growth, and targeting Cyclophilin A, while maintaining body weight.

Keywords: BAX/BCL-2 expression ratio, Cyclophilin A, DMBA-induced breast cancer, Doxorubicin, Molecular docking, *Spatholobus littoralis*

Introduction

One of the most common cancers and leading cause of death for woman is breast cancer [1]. Despite advances in therapeutic strategies, the effectiveness of chemotherapy remains limited due to drug resistance and systemic toxicity [2]. Doxorubicin, a widely used chemotherapeutic agent, remains primary agent of breast cancer treatment; however, its clinical effectiveness is often hindered by chemoresistance and dose limiting side effects [3]. Therefore, the development of effective adjuvant strategies to enhance chemosensitivity and improve therapeutic outcomes is urgently needed [4]. Apoptosis plays a critical role in maintaining cellular homeostasis and represents a key target in cancer therapy. Dysregulation of apoptosis is one of the major mechanisms underlying therapeutic resistance [5]. Under normal conditions, apoptosis regulates cell proliferation, whereas its disruption is a hallmark of malignancy, including breast cancer [6,7]. The apoptosis process is primarily regulated by the balance between pro-apoptosis and anti-apoptosis proteins, particularly BAX and BCL-2 [8,9]. Decreased expression of BAX and increased expression of BCL-2 have been associated with chemoresistance and poor prognosis [10]. Therefore, modulation of the BAX/BCL-2 expression ratio represents a promising therapeutic strategy to enhance apoptosis response in cancer treatment. In addition to BAX/BCL-2 ratio, upstream regulators of apoptosis signaling have gained increasing attention, such as Cyclophilin A (CypA) [11].

CypA is a member of the immunophilin family with peptidyl-prolyl cis-trans isomerase (PPIase) activity and is ubiquitously expressed in various cell types [12,13]. This protein meditates a wide range of biological functions, including signal transduction, gene expression, mitochondrial function, and cellular protection against oxidative stress [14,15]. One of its key mechanisms involves interaction with apoptosis signal-regulating kinase 1 (ASK1), which can activate the JNK and p38MAPK pathways under stress conditions [16-18]. Studies suggest that CypA may inhibit ASK1 activation, thereby suppressing downstream apoptosis signaling and promoting cell survival. Activation of ASK1 leads to phosphorylation of JNK and p38, subsequently inducing caspase-3 activation and apoptosis [19]. Studies have demonstrated that CypA can inhibit the phosphorylation of ASK1 at *Ser966*, thereby suppressing the activation of the JNK and p38 pathways. This physical interaction between CypA and ASK1 acts as a negative regulatory mechanism of apoptosis signaling, rendering CypA a cytoprotective factor in various pathological conditions, including cancer and degenerative diseases [20]. In this context, evaluating the binding affinity of *S. littoralis* compounds toward Cyclophilin A may help to elucidate their potential mechanism in regulating apoptosis related pathways. Therefore, targeting Cyclophilin A through *in silico* analysis represents a relevant approach to complement *in vivo* findings on apoptosis regulation.

Combination therapy involving chemotherapeutic agents and natural bioactive compounds has gained increasing attention due to its potential to overcome drug resistance and minimize toxicity. The ethanolic extract of *Spatholobus littoralis* (S. *littoralis*) has been reported to contain flavonoids and polyphenols with cytotoxic, antioxidant, and pro-apoptosis activities [21,22]. Previous studies have highlighted the potential of bioactive compounds from this plant to interact with apoptosis-regulating proteins [23]. *S. littoralis* is a plant originating from Kalimantan, the roots of this plant are used as a cancer medicine and anti-inflammatory by the local people. *Liquid chromatography-mass spectrometry/mass spectrometry* (LC-MS/MS) based profiling enables comprehensive identification of bioactive compounds in plant extracts, allowing prediction of their biological activity against specific molecular targets [24]. Evaluation of BAX and BCL-2 gene expression using qRT-PCR in tumor tissues provides direct insight into the effect of the combination of *S. littoralis* extract and doxorubicin on apoptosis regulation. The DMBA (7,12-dimethylbenz[a]anthrac ene)-induced rat model serves as an established experimental model for studying breast carcinogenesis, as it closely mimics the histopathological characteristics of human breast cancer [25].

Previous studies have primarily focused on either upstream or downstream components of apoptosis signaling in isolation, and have largely evaluated natural compounds as single agents rather than in combination with established chemotherapeutic drugs [26-28]. However, doxorubicin remains a standard and widely used agent in breast cancer therapy, and its efficacy is often limited by chemoresistance [29]. To date, no study has comprehensively integrated upstream molecular

targeting and downstream apoptosis gene regulation to evaluate the mechanistic basis of combination therapy involving *S. littoralis* extract and doxorubicin. This is the first to investigate the combined effects of *S. littoralis* extract and doxorubicin on apoptosis regulation thru an integrated approach involving the upstream molecular targeting of Cyclophilin A *in silico* study and the downstream expression analysis of BAX/BCL-2 genes in a DMBA-induced breast cancer in rats model. This integrated approach thru *in silico* and *in vivo* studies supports the potential development of adjuvant therapy that can overcome chemoresistance thru a combination-based natural compound approach. We hypothesize that the combination of S. *littoralis* extract and doxorubicin enhances chemotherapy sensitivity by inhibiting survival signals mediated by Cyclophilin A *in silico* study, thereby increasing the BAX/BCL-2 ratio, and ultimately promoting apoptosis in DMBA-induced breast cancer in rats model.

This study aims to evaluate the effects of *S. littoralis* extract combined with doxorubicin on apoptosis regulation, particularly the BAX/BCL-2 expression ratio, in a DMBA-induced breast cancer rat model, and to investigate the interaction of its major compound with Cyclophilin A through molecular docking analysis. It is hypothesized that the combination treatment enhances apoptosis activity by modulating the BAX/BCL-2 expression ratio and that its bioactive compound exhibits a favorable interaction with Cyclophilin A.

Materials and methods

Extraction and characterization of *S. littoralis*

A total of 7 kg of *Spatholobus littoralis* roots were collected as raw material. After drying and grinding into a fine powder, the weight was reduced to 4.13 kg. The powder material was maceration using ethanol as the solvent, resulting in a final yield of 1.39 kg of *S. littoralis* ethanolic extract. Extraction was performed by maceration with 96% ethanol for 3×24 h with occasional stirring. The obtained filtrate was filtered and then evaporated using a rotary evaporator at < 50 °C to yield a concentrated extract. The extract was stored at 4 °C in a dark container until use. The extract was characterized using LC-MS/MS analysis. The analysis was performed on an Ultra-Performance Liquid Chromatography (UPLC) unit coupled with a Xevo G2-S QTof mass spectrometer (ACQUITY UPLC® H-Class System, Waters, USA). Separation was carried out using a C18 column (1.8 µm particle size; 2.1 × 100 mm, ACQUITY UPLC® HSS, Waters, USA) at a column temperature of 50 °C and room temperature of 25 °C. The mobile phases consisted of Phase A: water + 5 mM ammonium formate, and Phase B: acetonitrile + 0.05% formic acid, with a flow rate of 0.2 mL/min using a stepwise gradient over 23 min. The sample injection volume was 5 µL, and samples were filtered through a 0.2 µm syringe filter prior to analysis [30].

In silico analysis

Compounds identified from the *S. littoralis* extract using LC-MS/MS analysis were subjected to *in silico* molecular docking to evaluate their binding affinity toward Cyclophilin A (CypA). Docking simulations were performed using Molegro Virtual Docker (MVD v7.0.0). The 3-dimensional crystal structure of Cyclophilin A (PDB ID: 3RDD) was retrieved from the RCSB Protein Data Bank (RCSB PDB). Water molecules (HOH) were removed from the protein structure prior to molecular docking using MVD. Polar hydrogen atoms were added, and the protein structure was energy-minimized to prepare it for docking analysis. Ligand structures were optimized by energy minimization using the "Ligand Energy Inspector" feature in MVD to ensure the most stable conformations. The docking protocol was validated by redocking the native ligand, and the simulation was considered valid when the RMSD value was less than 2 Å. Each docking run was replicated 20 times to confirm the reproducibility of binding poses. The resulting ligand-protein interactions were analyzed based on energy parameters, including the MolDock Score, Hydrogen Bond (H-bond) energy, and Rerank Score, with the Rerank Score used as the primary criterion for ranking binding affinity. Compounds exhibiting the lowest Rerank Scores were selected for further pharmacokinetic and drug-likeness evaluation. The pharmacokinetic properties were predicted according to Lipinski's Rule of Five, while ADME/T (absorption, distribution, metabolism, excretion, and toxicity) profiles were estimated using the SwissADME (http://www.swissadme.ch/index.php) and pkCSM (https://biosig.lab.uq.edu.au/) web servers. The predicted parameters were compared with the reference

drug Doxorubicin to assess the therapeutic potential of S. *littoralis*-derived compounds as combination therapy candidates targeting Cyclophilin A.

***In vivo* study**

This research protocol has been approved by the Ethics Committee of the Faculty of Medicine, University of Indonesia, and received a certificate of passing ethical review on January 19, 2024 with No. KET- 105 / UN2.F1 / ETIK / PPM.00.02 /2024. Female Sprague-Dawley rats (6 - 8 weeks old, ± 200 g) were obtained from BPOM. Breast cancer was induced orally using 7,12-dimethylbenz(α)anthracene (DMBA) at 20 mg/kg body weight twice weekly for 11 doses until tumor nodules with volumes ≥ 3 - 5 cm^3 formed. The initial nodules are first palpable and can be measured in the week 4 following the final DMBA induction. Tumor growth reached a volume of approximately 3 - 5 cm^3 within 2 - 3 weeks after the initial nodule detection. These findings indicate variability in tumor onset and progression among individual animals. This observation is the same as from previous reports, which showed tumor nodule appearance at week 4 and week 6 [31,32]. However, such variability is commonly reported in DMBA-induced breast cancer models, depending on factors such as dosage, frequency of administration, and individual biological responses. Animals were randomly divided into 7 treatment groups: (1) normal (2) cancer control (DMBA without therapy), (3) doxorubicin 5 mg/kg body weight once weekly i.p., (4 - 6) combination of doxorubicin with extract at doses of 100, 200, and 400 mg/kg body weight, respectively, and (7) extract alone at 400 mg/kg body weight. Doses were determined based on a preliminary acute toxicity study (limit test, OECD 425) conducted in Sprague Dawley rats, in which the LD_{50} of *S.littoralis* extract was estimated to be > 5,000 mg/kg body weight, with no mortality, minimal clinical signs, and no significant abnormalities observed during necropsy [33]. Accordingly, the extract was classified as non-toxic based on the Indonesian National Agency of Drug and Food Control (BPOM) Regulation No. 7/2014 [34]. Based on these findings, the experimental doses were selected using fractionated levels of the maximum safe dose (1/50, 1/25 and 1/12.5), resulting in doses of 100, 200, and 400 mg/kg body weight, respectively. These doses fall within a safe sub-chronic range and were considered appropriate to ensure safety while maintaining potential therapeutic efficacy. The sample size per group was determined according to Federer's formula for experimental design, which requires a minimum of 4 animals per group (n = 4) to ensure adequate statistical power. Treatments were administered for four weeks. At the end of the treatment, animals were euthanized, and tumor tissues were collected and stored at −80 °C for molecular analysis. Tumor volume was calculated using the following formula: $V = 0.5 \times L \times W^2$, where V represents tumor volume, L is tumor length, and W is tumor width [35]. Tumor growth inhibition (TGI) was determined based on changes in tumor volume between the treatment groups and the control group during the treatment period. After obtaining the initial and final tumor volume data, the TGI value was calculated using the following formula [36]:

$$\%TGI = \left[1 - \frac{\Delta V_{\text{treatment}}}{\Delta V_{\text{control}}}\right] \times 100\%$$

where ΔV treatment represents the change in tumor volume in the treatment group, and ΔV control represents the change in tumor volume in the DMBA control group [37].

qRT-PCR analysis

Total RNA was extracted from tumor tissues using RNA Extraction Reagent (Vazyme, China) according to the manufacturer's instructions. RNA concentration and purity were measured using a NanoDrop 2000C UV-VIS spectrophotometer (Thermo Fisher Scientific, USA). RNA quality was evaluated based on an A260/280 ratio of 1.8 - 2.0, an A260/230 ratio > 1.8, and an 18S/28S rRNA ratio of 1.8 - 2.1 as criteria for qPCR suitability. cDNA synthesis was performed using HiScript II Q RT SuperMix for qPCR (+gDNA wiper, Vazyme, China) according to the manufacturer's protocol, including genomic DNA removal and reverse transcription in a single reaction tube. Gene expression analysis was conducted using ChamQ SYBR qPCR Master Mix (Vazyme, China) on a Real-Time Quantitative Thermal Cycler (Vazyme, Model FMR3). The instrument software was used to program PCR cycles, monitor amplification curves, and calculate relative gene expression using the ΔΔCt method.

Primers used were: BAX: forward 5'-GTCTCAG GCGAATTGGCGAT-3'; reverse 5'-TAGGAAAGG AGGCCATCCCAG-3'. BCL-2: forward 5'-TGTGGAT GACTGACTACCTGAACC-3'; reverse 5'-CAGCCAG GAGAAATCAAA CAGAGG-3'. β-actin: forward 5'-GTCTCAGGCGAATTGGCGAT-3'; reverse 5'-TAGG AAAG GAGGCCATCCCAG-3'. the qRT-PCR thermal cycling condition for all reactions was 95 °C for 30 min, followed by 40 cycles of 94 °C for 30 s, and 60 °C for 30 s. Each experimental group included n = 4 biological replicates, and each biological sample was measured in technical duplicate. Gene expression levels of BAX and BCL-2 were normalized to the housekeeping gene β-actin using the ΔΔCt method, with the mean Ct value of the technical duplicates used for analysis [38].

Statistical analysis

Gene expression analysed using GraphPad Prism 10.6.1 Software (GraphPad Software Inc., La Jolla, CA, USA) and presented as the means ± SD (n = 4). Difference between samples were performed using ANOVA with probability values of significant differences, where normal control is compared with DMBA group and #$p < 0.05$ is considered significant. the tested group is compared with DMBA Control and *$p < 0.05$ was significant.

Results and discussion

Extraction and characterization *Spatholobus littoralis*

Maceration with ethanol 96% yielded 1.394 kg of a thick, dark brown extract with a strong characteristic aroma. The extraction produced a 24% yield, calculated from the ratio of the ethanol extract to the powdered simplicia. The LC-MS/MS results in **Table 1** identified 23 secondary metabolite compounds found in the ethanol extract of S. *littoralis*. The most frequently identified secondary metabolites were phenolic and flavonoid groups.

Table 1 Docking results of compounds identified from LC-MS/MS analysis against cyclophilin A compared with the native ligand EA4_166.

No	Compound	Molecular weight (g/mol)	Molecular Formula	Ligand pose and (CID)	MolDock Score (kJ/mol)	Rerank Score (kJ/mol)	HBond (kJ/mol)
00	**Native Ligand**			[00]EA4_166[A]	−104.219	−91.340	−4.711
00	Doxorubicin	543.52	$C_{27}H_{29}NO_{11}$	[03]31703	−74.234	−70.795	−7.918
1	N-2-[4-(3,3 Dimethylallyloxy)phenyl]ethylcinnamide	335.4	$C_{22}H_{25}NO_2$	[00]131750978	−134.932	−110.618	−1.526
2	Glycyroside	562.5	$C_{27}H_{30}O_{13}$	[01]101939210	−127.271	−108.225	−11.968
3	Paprazine	283.32	$C_{17}H_{17}NO_3$	[00]5372945	−125.109	−104.000	−6.007
4	Benzamide, 4-methyl-N-[(phenylamino)carbonyl]	254.28	$C_{15}H_{14}N_2O_2$	[01]280343	−111.997	−99.155	−7.793
5	N-Formylanonaine	293.3	$C_{18}H_{15}NO_3$	[00]158516	−111.342	−89.111	−2.224
6	Trihydroxychalcone	256.25	$C_{15}H_{12}O_4$	[05]638278	−103.654	−88.959	−6.698
7	Syringaresinol	418.4	$C_{22}H_{26}O_8$	[00]100067	−114.316	−88.677	−5.669
8	Lupinalbin A	284.22	$C_{15}H_8O_6$	[00]5324349	−103.101	−86.117	−2.992
9	Butin	272.25	$C_{15}H_{12}O_5$	[02]92775	−94.590	−83.345	−3.043
10	Thiosildenafil	490.6	$C_{22}H_{30}N_6O_3S_2$	[00]10228242	−121.173	−81.565	−4.440
11	Uridine	244.2	$C_9H_{12}N_2O_6$	[00]6029	−97.397	−81.289	−12.348
12	Maackiain	284.26	$C_{16}H_{12}O_5$	[00]91510	−98.970	−78.567	−4.321

No	Compound	Molecular weight (g/mol)	Molecular Formula	Ligand pose and (CID)	MolDock Score (kJ/mol)	Rerank Score (kJ/mol)	HBond (kJ/mol)
13	8-O-methylretusin	298.29	$C_{17}H_{14}O_5$	[00]5319771	−86.400	−76.731	−1.228
14	Columbamine	338.4	$C_{20}H_{20}NO_4$	[02]72310	−88.240	−76.437	−3.497
15	N-Butylbenzenesul fonamide	213.3	$C_{10}H_{15}NO_2S$	[00]19241	−87.739	−75.622	−5.321
16	Berberine	336.4	$C_{20}H_{18}NO_4$	[02]2353	−99.429	−75.179	−4.147
17	Daidzein	254.24	$C_{15}H_{10}O_4$	[00]5281708	−84.778	−74.794	−2.500
18	Visnadine	388.4	$C_{21}H_{24}O_7$	[00]442151	−100.503	−72.353	−4.845
19	Genistein	268.26	$C_{16}H_{12}O_4$	[02]5280378	−80.183	−71.845	−1.085
20	Cycloeucalenol	426.7	$C_{30}H_{50}O$	[03]101690	−92.193	−60.560	0.000
21	Isoquinoline	129.16	C_9H_7N	[01]8405	−66.413	−58.733	−4.443
22	Procyanidin	594.5	$C_{30}H_{26}O_{13}$	[00]107876	−96.507	−3.296	−10.827
23	Dihydrocucurbitacin	520.7	$C_{30}H_{48}O_7$	[03]11504572	−43.121	102.888	0.611873

The LC-MS/MS characterization reveals a distinct dominance of phenolic derived metabolites in S. *littoralis,* particularly flavonoids, isoflavones, and polyphenols. This characteristic profile highlights the biochemical uniqueness of Fabaceae plants in producing a wide range of phenolic compounds through the phenylpropanoid pathway [39]. We found that among the 23 identified compounds, the phenolic derivatives included trihydroxychalcone, butin, procyanidin, lupinalbin A, maackiain, 8-O-methylretusin, daidzein, N-2-[4-(3,3-dimethylallyloxy)phenyl]ethylcinnamide, visnadine, and formono-netin. We also found several alkaloids such as paprazine, columbamine, glycyroside, and berberine. The phenylpropanoid pathway produces the precursor p-coumaroyl-CoA which is then processed through the action of the enzymes CHS, CHI, and IFS into various flavonoids and isoflavonoids [40,41]. These compounds function as defense metabolites (phytoalexins), so they are biologically abundant. The activity of oxygenase, methyltransferase, and glycosyltransferase enzymes further enriches the variety of phenolic structures, making this group the dominant component in the extract [42].

Molecular docking analysis of Cyclophilin A inhibition by *Spatholobus littoralis* phytochemicals

Docking validation was performed using the re-docking method with the native ligand EA4_166 against the target protein Cyclophilin A (PDB ID: 3RDD). As shown in Table 1, the two best docking poses obtained showed RMSD values around 1.463 Å, which is below the validation threshold (< 2 Å).

Table 2 Validation results of native ligand EA4_166 docking against Cyclophilin A.

Pose	Ligand Name	MolDock Score (kJ/mol)	Rerank Score (kJ/mol)	RMSD (Å)	HBond (kJ/mol)
[03]EA4_166 [A]	EA4_166 [A	−100.885	−87.170	1.463	5.929
[00]EA4_166 [A]	EA4_166 [A	−111.598	−84.882	1.464	−12.329

The molecular docking results show in **Table 1** show that several compounds exhibit higher binding affinity toward Cyclophilin A compared to the native ligand EA4_166 [A] (MolDock Score –104.219; Rerank Score –91.340). The ligand 131750978 showed the best binding pose with a MolDock Score of –134.932 and Rerank Score of –110.618, followed by 101939210 (MolDock Score –127.121; Rerank Score –108.225). Other compounds, such as 5372945 and 280343, also demonstrated competitive docking scores, indicating lower binding energies than the control ligand. Some compounds displayed relatively weak interactions, such

as ligand 11504572, which had a MolDock Score of –43.121 and a positive Rerank Score of 102.888. Particularly ligands with the lowest energy scores, such as 131750978 and 101939210.

Figure 1 Illustrates the ligand-binding location within the active pocket of Cyclophilin A (highlighted in green), along with the interacting amino acid residues. Panel (a) shows the native ligand EA4_166 [A], which interacts with key residues of Cyclophilin A, including Ala101, Asn102, Gly72, Gln63, Arg55, and Thr107. This interaction pattern produced a Rerank Score of –91.340 kJ/mol, serving as a reference for docking method validation. In contrast, Panel (b) shows the test compound (CID 131750978), which forms interactions with critical residues such as Asn102, Gly72, Gly74, Ser110, Gln111, Thr107, and Gln63. The more diverse hydrogen-bonding network observed in the test compound contributes to a lower Rerank Score (–110.618 kJ/mol) compared to the native ligand, indicating stronger binding affinity and greater complex stability. With its improved binding energy and specific interactions at the active-site residues, the test ligand (CID 131750978) demonstrates strong potential as a Cyclophilin A inhibitor.

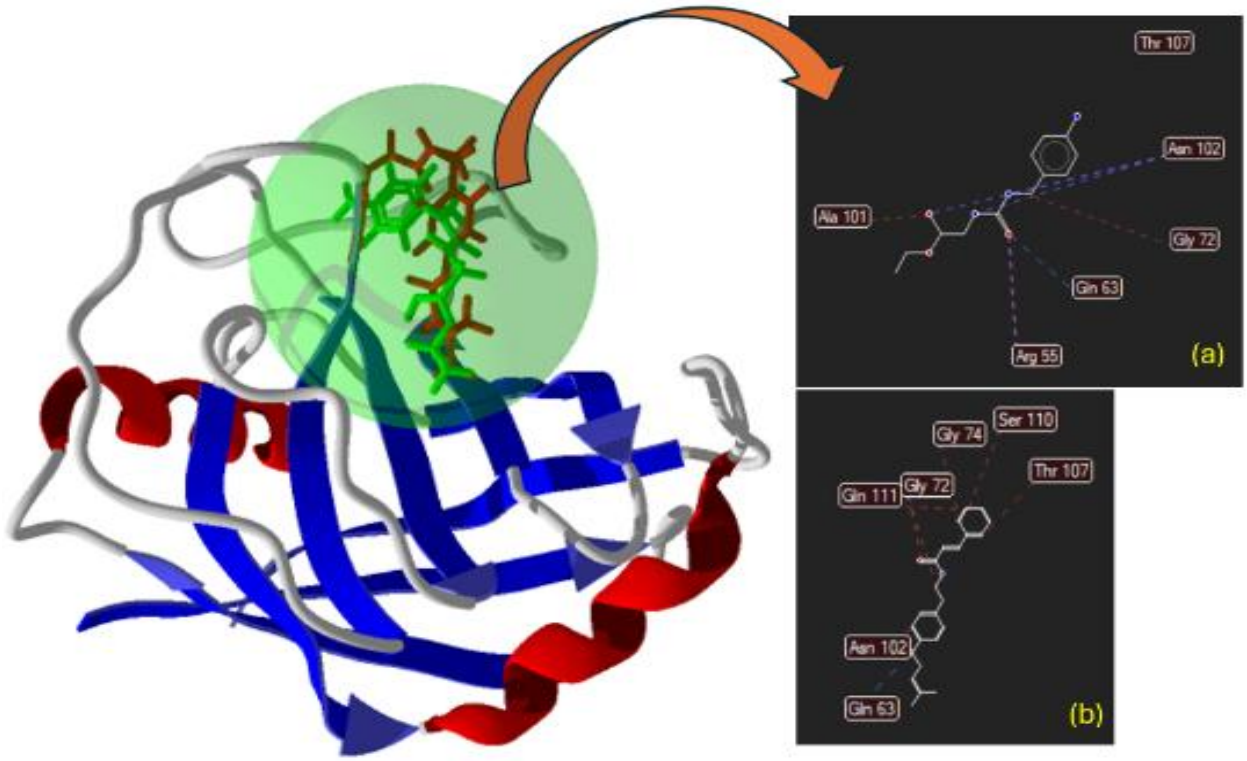

Figure 1 Interaction of the native ligand and test compound (CID 131750978) with the binding pocket of Cyclophilin A (CypA) based on molecular docking analysis. three-dimensional visualization of ligand binding within the CypA active site (green sphere), along with 2-dimensional interaction diagrams showing key amino acid residues: (a) native ligand and (b) test compound.

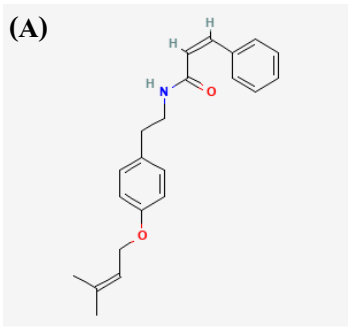

N-2-[4-(3,3 Dimethylallyloxy)phenyl]ethylcinnamide

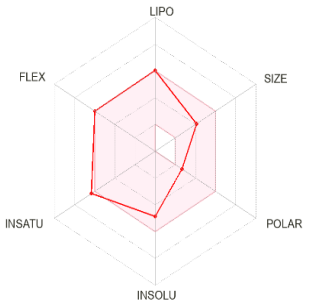

Descriptor	Value
Molecular Weight	335.447
LogP	4.4037
#Rotatable Bonds	8
#Acceptors	2
#Donors	1
Surface Area	149.584

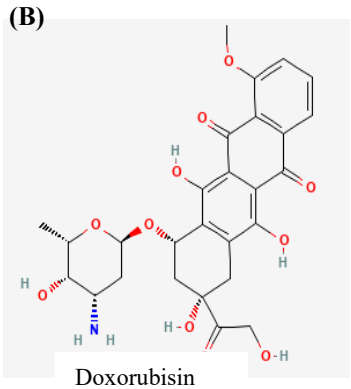

Doxorubisin

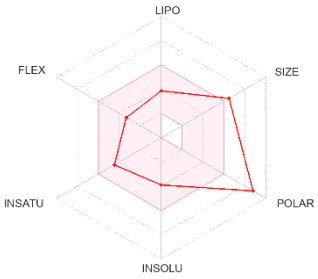

Molecular Weight	543.525
LogP	0.0013
#Rotatable Bonds	5
#Acceptors	12
#Donors	6
Surface Area	222.081

Figure 2 Bioavailability score prediction and drug likeliness properties of (A) N-2-[4-(3,3 Dimethylallyloxy) phenyl]ethylcinnamide and (B) Doxorubicin using SwissADME. The chemical structures, bioavailability radar plots, and key physicochemical parameters including molecular weight, lipophilicity (LogP), hydrogen bond donors and acceptors, rotatable bonds, and topological polar surface area are presented.

The physicochemical analysis (**Figure 2**) showed that the compound N-2-[4-(3,3-dimethylallyloxy) phenyl]ethylcinnamide had a molecular weight of 335.45 g/mol, LogP value of 4.40, 8 rotatable bonds, 2 hydrogen bond acceptors, 1 hydrogen bond donor, and a polar surface area (PSA) of 149.58 Å². According to these parameters, the compound satisfies all criteria of Lipinski's Rule of Five, although its polar surface area slightly exceeds the optimal threshold (< 140 Å²).In contrast, doxorubicin possesses a molecular weight of 543.52 g/mol, LogP of 0.0013, five rotatable bonds, twelve hydrogen bond acceptors, six hydrogen bond donors, and a polar surface area of 222.08 Å². These parameters indicate that doxorubicin violates three key criteria of Lipinski's Rule of Five and displays high polarity, which may contribute to its poor oral bioavailability.

Cyclophilin A (CypA) is known not only as a cyclosporin-binding protein but also as a key mediator in regulating oxidative stress and inflammatory signaling. The activation of CypA triggers downstream signaling pathways involving stress-activated protein kinases (SAPKs), particularly JNK (c-Jun N-terminal kinase) and p38 MAPK. These pathways are regulated by apoptosis signal-regulating kinase 1 (ASK1), an upstream kinase responsible for responding to oxidative stress and proinflammatory cytokines [43]. Under cellular stress conditions, the interaction of CypA with ASK1 activates JNK and p38 MAPK, thereby stimulating the expression of pro-apoptosis genes. Activation of JNK/p38 enhances the expression of BAX (pro-apoptosis) while suppressing BCL-2 (anti-apoptosis) expression. The alteration of the BAX/BCL-2 ratio increases mitochondrial membrane permeability, promotes cytochrome c release, and activates caspase cascades, ultimately leading to apoptosis [44]. Thus, modulation of CypA such as through specific inhibitors may disrupt ASK1-JNK/p38 activation and rebalance

BAX and BCL-2 expression. This mechanism highlights the potential of CypA inhibition as a therapeutic strategy to regulate excessive apoptosis in degenerative or chronic inflammatory diseases [45]. The main novelty of this study lies in the simultaneous evaluation of *in vivo* biological effects and *in silico* analysis of the active compounds of *S. littoralis*. This reseach reports demonstrating that the combination of *S. littoralis* extract and doxorubicin not only induces downregulation of the anti-apoptosis gene BCL-2 and upregulation of the pro-apoptosis gene BAX, but also modulates the expression of Cyclophilin A, a key mediator of oxidative stress involved in the activation of the ASK1-JNK/p38 MAPK pathway.

In silico analysis of bioavailability and drug-likeness parameters using SwissADME (**Figure 2**) showed a marked difference between N-2-[4-(3,3-dimethylallyloxy)phenyl] ethylcinnamide and doxorubicin in terms of pharmacokinetic potential and biological permeability. The compound N-2-[4-(3,3-dimethylallyloxy)phenyl]ethylcinnamide has a molecular weight of 335.45 g/mol, LogP of 4.40, 2 hydrogen bond acceptors, 1 donor, 8 rotatable bonds, and a topological polar surface area (TPSA) of 149.58 Å². According to Lipinski's Rule of Five, the compound satisfies all major parameters of drug-likeness molecular weight < 500, LogP < 5, and hydrogen bond donors/acceptors < 5/10 [46]. The relatively high LogP value indicates good lipophilicity, suggesting optimal cell membrane permeability. A TPSA <150 Å² also implies high oral absorption and good membrane penetration potential [47]. Conversely, doxorubicin has a molecular weight of 543.52 g/mol, LogP of 0.0013, 12 acceptors, 6 donors, and TPSA of 222.08 Å². These parameters indicate that doxorubicin does not fully comply with Lipinski's criteria, mainly due to its large molecular weight and high polarity. This explains its low oral bioavailability and dependence on intravenous administration in clinical use [48]. A LogP near zero reflects amphiphilic properties, enabling interaction with both hydrophilic and lipophilic components of the cell membrane, but with limited tissue distribution due to strong plasma protein binding and low permeability [49]. Based on the bioavailability radar plot, N-2-[4-(3,3-dimethylallyloxy)phenyl]ethylcinnamide showed a more balanced profile in lipophilicity, molecular size, flexibility, and polarity, indicating a superior pharmacokinetic profile compared to doxorubicin. Doxorubicin exhibited a wider radar area in polarity and insolubility, reflecting limited oral absorption and membrane diffusion [50]. These findings suggest that N-2-[4-(3,3-dimethylallyloxy)phenyl]ethylcinnamide has potential as an adjuvant compound to enhance the therapeutic efficacy of doxorubicin, with favorable drug-likeness and bioavailability profiles.

Antitumor effects on DMBA-induced breast cancer rat model

Rat body weight profiles

Changes in body weight during the experimental period are shown in **Figure 3**. Overall, the healthy group exhibited a steady increase in body weight from week 0 to week 4. In contrast, the DMBA-induced group showed a tendency toward reduced or stagnant body weight over time, indicating metabolic disturbances associated with tumor progression. The group treated with doxorubicin (DOX) demonstrated a more pronounced decrease in body weight compared to the DMBA group, particularly from week 2 to week 4, with statistically significant differences ($p < 0.05$). This finding suggests the presence of systemic toxicity induced by chemotherapy. In contrast, the combination treatment groups (Adj1, Adj2, and Adj3) showed relatively more stable body weight profiles compared to the DOX group. Notably, the Adj3 group maintained body weight close to baseline levels throughout the experimental period without significant decline. The group treated with S. *littoralis* extract also exhibited a stable body weight profile comparable to the healthy group.

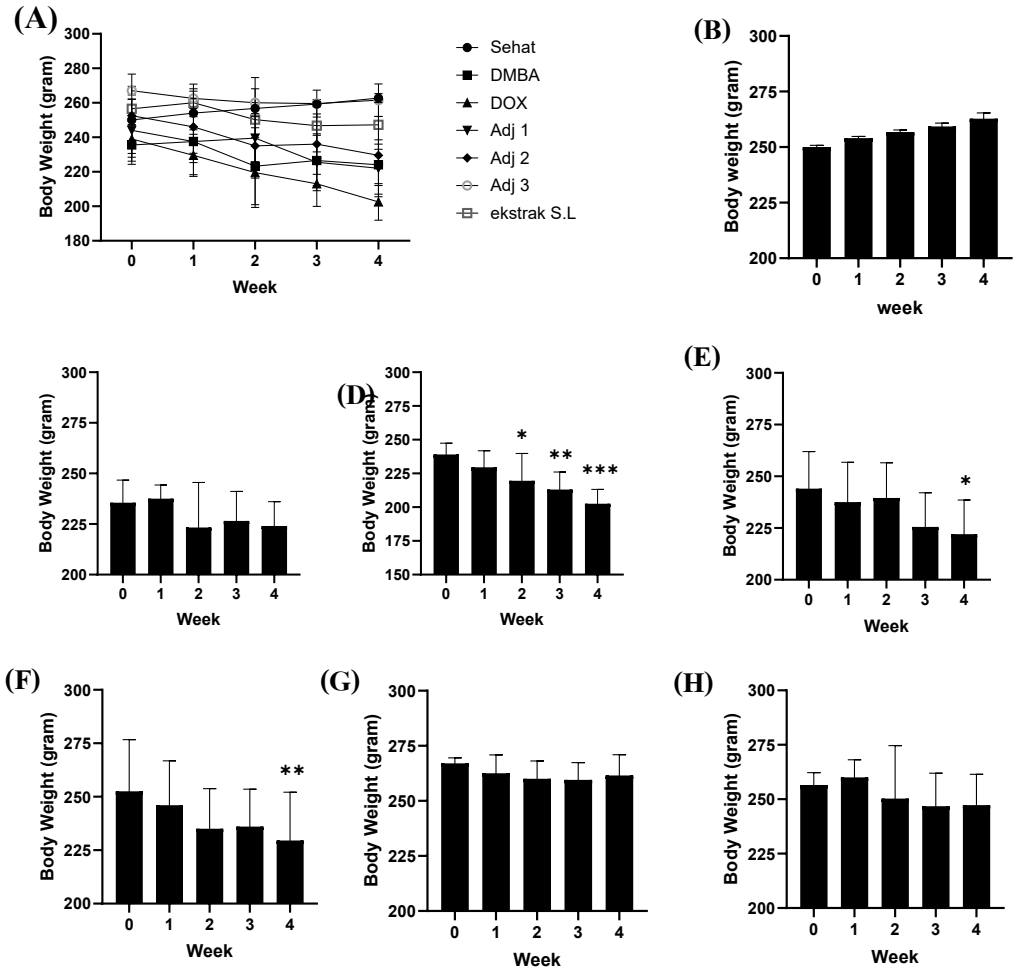

Figure 3 Body weight profile and mean body weight comparison in each treatment group per week. (A) Body weight profile of all experimental groups, (B) Body weight of normal group, (C) Body weight of DMBA group, (D) Body weight of DOX group, (E) Body weight of Adj1 group, (F) Body weight of Adj 2 group, G: Body weight of Adj 3 group, H: Body weight of S.L group. Data are presented as mean ± SEM and analyzed using a mixed-effects model (REML) with repeated measures, followed by multiple comparisons test. Significant differences are indicated as * ($p \leq 0.05$), ** ($p \leq 0.01$), *** ($p \leq 0.001$).

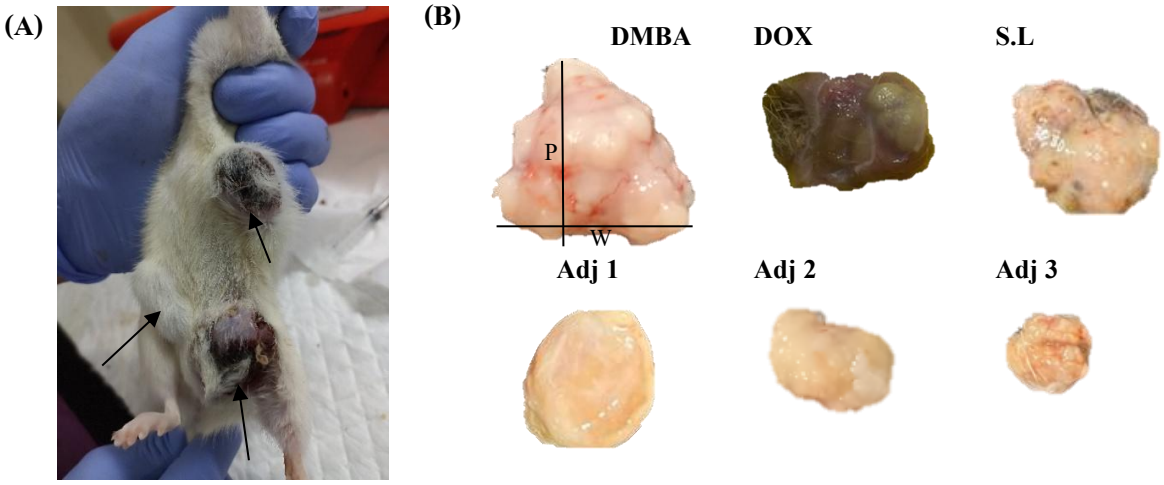

Figure 4 Mammary carcinoma nodules that occurred in DMBA-induced rats and mammary carcinoma volume in each group after necropsy. (A) Sprague Dawley rats showing several mammary tumor nodules after DMBA induction (arrows indicate tumor locations). (B) Comparison of mammary tumor volume in various treatment groups after necropsy.

DMBA control group displayed the largest nodules, while Adj3 combination treatment showed the smallest tumor size. Statistical analysis was performed using 1-way ANOVA followed by Tukey's post hoc test ($p < 0.05$). Quantitative volume measurements before and after treatment, along with Tumor Growth Inhibition (%TGI) percentages, are presented in **Table 3**. DMBA control exhibited tumor volume progression from 4.17 to 7.34 cm^3 (%TGI = 0%), whereas DOX, Adj1, Adj2, Adj3, and SL treatment groups demonstrated volume reduction, with Adj3 achieving the highest inhibition at 98.14% TGI.

Table 3 Nodule volume and percentage of tumor growth inhibition in each group during the 4-week treatment.

Group	Pre-Treatment Volume (V1) (cm^3)	Post- treatment Volume (V2) (cm^3)	RTV (V2/V1)	%TGI
DMBA	4.17	7.34	1.760	0.00
DOX	6.1	1.9	0.311	90.17
Adj 1	5.2	0.7	0.135	95.75
Adj 2	5.1	0.4	0.078	97.53
Adj 3	5.1	0.3	0.059	98.14
S.L	5.2	3.4	0.654	79.37

Gen expression analysis of BCL-2 and BAX by quantitative real-time PCR

Gene expression analysis of BCL-2 and BAX demonstrated that DMBA-induced carcinogenesis significantly upregulated anti-apoptosis BCL-2 expression compared to normal control (1.31 - 1.53 vs 1.00; $p < 0.05$). Conversely, pro-apoptosis BAX expression in the DMBA group was significantly downregulated (0.428 - 0.540; $p < 0.05$), indicating a molecular shift toward anti-apoptosis dominance that promotes tumor cell survival. Doxorubicin monotherapy induced substantial BCL-2 suppression (0.11 - 0.18; $p < 0.05$ vs DMBA) accompanied by significant BAX upregulation (1.39 - 1.55; $p < 0.05$ vs DMBA), signifying intrinsic apoptosis pathway activation via DNA damage. Combination therapy groups (ADJ) exhibited dose-dependent responses, with ADJ 3 producing the most potent effect through

maximal BCL-2 inhibition (0.03 - 0.09; $p < 0.05$ vs DMBA) and highest BAX elevation (2.01 - 2.36; $p < 0.05$ vs DMBA). *Spatholobus littoralis* (S.L.) monotherapy effectively suppressed BCL-2 (0.01 - 0.05; $p < 0.05$ vs DMBA), although BAX upregulation approximated normal control levels (0.92 - 1.02). The relative expression of BCL-2 and BAX genes, as well as the BCL-2/BAX ratio and tumor nodule volume, are presented in **Figure 5**.

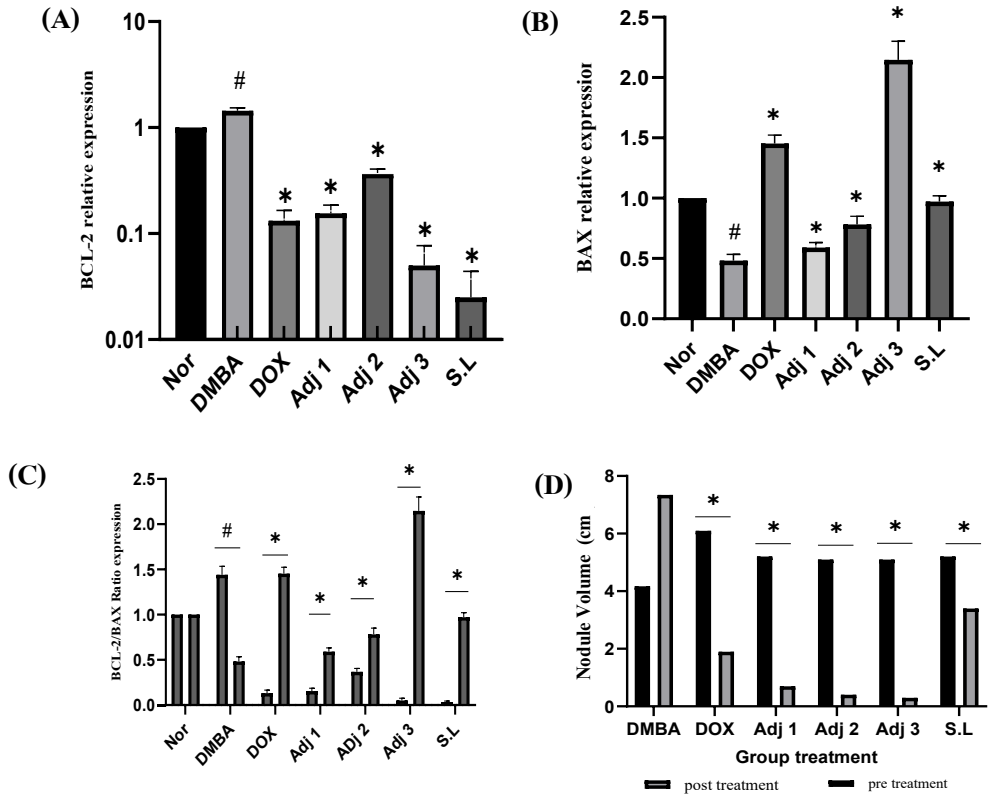

Figure 5 Relative expression of BCL-2 genes, BAX genes, BCL-2/BAX ratio, and tumor nodule volume in DMBA-Induced Breast Cancer Rats Under Different Treatments. (A) BCL-2 gene expression; (B) BAX gene expression; (C) BCL-2/BAX ratio; and (D) tumor nodule volume. NOR represents the normal control; DMBA serves as the negative control (20 mg/kg body weight, dissolved in corn oil, administered 11 times); DOX represents the positive control (doxorubicin, 5 mg/kg body weight). Adj1, Adj2, and Adj3 groups were treated with a combination of *Spatholobus littoralis* extract and doxorubicin at doses of 100, 200, and 400 mg/kg body weight, respectively; S.L group received *S. littoralis* extract alone at 400 mg/kg body weight. Data are presented as mean ± SEM; n = 4, Statistical analysis was performed using one-way analysis of variance (ANOVA), followed by a post hoc test. Statistical significance was defined as #$p < 0.05$ versus the normal control and *$p < 0.05$ versus the DMBA group.

The increased BCL-2/BAX ratio observed in the DMBA group indicates a dominant anti-apoptosis effect due to DMBA-induced carcinogenesis. DMBA activation in the liver thru CYP1A1 and CYP1B1 produces reactive epoxide intermediates that form DNA adducts and trigger oncogenic mutations [51]. The research results indicate that the therapy administered significantly suppresses tumor growth and is believed to work thru specific molecular mechanisms, as evidenced by the integration of *in vivo* and *in silico* data. Overall, the combination group, particularly Adj3, demonstrated higher antitumor efficacy and a better safety profile compared to monotherapy. This is evidenced by a more significant reduction in tumor volume and a higher percentage of tumor growth inhibition (%TGI) compared to the doxorubicin group, which effective in suppressing the tumor, still shows limitations in terms of systemic toxicity. Doxorubicin effectively suppresses

tumor growth by intercalating DNA and inhibiting topoisomerase II, but its systemic toxicity often leads to significant weight loss (BW) thru cachexia and reduced food intake. This weight loss, observed as a 13% loss in a rat model over 15 days, correlates with sarcopenia (10% - 20% muscle mass reduction) and can disrupt the overall treatment efficacy even tho the tumor is inhibited [52,53].

While doxorubicin reduces tumor volume, for example, in the DIO breast cancer xenograft, weight loss due to multi-organ toxicity limits the cumulative dose of doxorubicin [54]. This weight loss is generally associated with chemotherapy side effects, such as gastrointestinal disturbances, decreased appetite, and increased oxidative stress that can trigger cachexia [55]. On the other hand, the combination group showed a more significant reduction in tumor volume and a higher increase in %TGI, while being able to maintain a relatively stable body weight. This indicates that combination therapy is not only more effective but also more physiologically safe because it does not cause metabolic disturbances [56,57]. When combined with the DNA-damaging effects of doxorubicin, this dual inhibition amplifies mitochondrial membrane destabilization and caspase activation across multiple tumor [58]. Treatment with S. *littoralis* alone also resulted in a decreased BCL-2/BAX ratio and moderate tumor growth inhibition (%TGI 79.37%). Although the effect was less pronounced than that observed in the combination group, the data indicate intrinsic pro-apoptotic activity. Phytochemical constituents are known to modulate mitochondrial apoptosis by suppressing anti-apoptotic proteins and enhancing pro-apoptotic signaling, suggesting that *S. littoralis* may function as a potential chemosensitizing agent when used adjunctively [59]. Importantly, correlation analysis revealed a strong inverse association between %TGI and the BCL-2/BAX indicating that tumor regression was tightly linked to modulation of mitochondrial apoptotic balance. This finding reinforces the concept that the BCL-2/BAX axis represents a critical mechanistic determinant of therapeutic response in DMBA-induced multifocal mammary tumors [60].

The intrinsic apoptosis pathway is regulated by the balance between pro-apoptotic proteins BAX and anti-apoptotic proteins BCL-2. An increased BAX/BCL-2 ratio induces mitochondrial outer membrane permeabilization, resulting in cytochrome c release and caspase activation, culminating in programmed cell death. This mechanistic framework explains the observed tumor volume reduction, as apoptosis is selectively induced in tumor cells [61]. The strong binding affinity of active compounds to CypA in your *in-silico* results supports the hypothesis that modulation of CypA function can influence downstream apoptotic pathways. This suggests a mechanistic link between compound binding and the activation of pro-apoptotic signaling *in vivo* [62].

The strong interaction between the extract compounds and CypA is suspected to trigger the activation of the downstream CypA-ASK1-JNK1 pathway, which ultimately enhances pro-apoptotic signaling thru increased BAX expression and decreased BCL-2. The activation of this pathway provides a mechanistic basis for the observed increase in the BAX/BCL-2 ratio in the combination group. Thus, the antitumor effects observed in macroscopic parameters are likely mediated by targeted apoptosis activation thru these molecular pathways [63]. The increased efficacy observed with the 400 mg/kg combination dose is due to a higher concentration of active compounds in the tumor tissue, allowing for more optimal modulation of the BCL-2 family proteins. This higher dose enhances BAX expression and reduces BCL-2, triggering mitochondrial membrane permeabilization, cytochrome c release, and more complete activation of the apoptosis cascade compared to lower doses. As a result, the BAX/BCL-2 ratio is higher, tumor volume is reduced more significantly, and %TGI is increased. Dysregulation of BCL-2 family proteins, particularly the overexpression of anti-apoptotic members such as BCL-2, confers a survival advantage to cancer cells and serves as a mechanism of therapeutic resistance. Therefore, higher doses of pro-apoptotic agents or combination therapies that inhibit BCL-2 can enhance BAX/BAK activation and effectively induce apoptosis [64,65].

Therefore, the proposed molecular pathway illustrating the effects of the extract combination with doxorubicin is presented in **Figure 6**. It shows how the interaction of active compounds with Cyclophilin A (CypA) activates the ASK1-JNK1 pathway, modulates the BAX/BCL-2 ratio, and ultimately induces selective apoptosis in tumor cells.

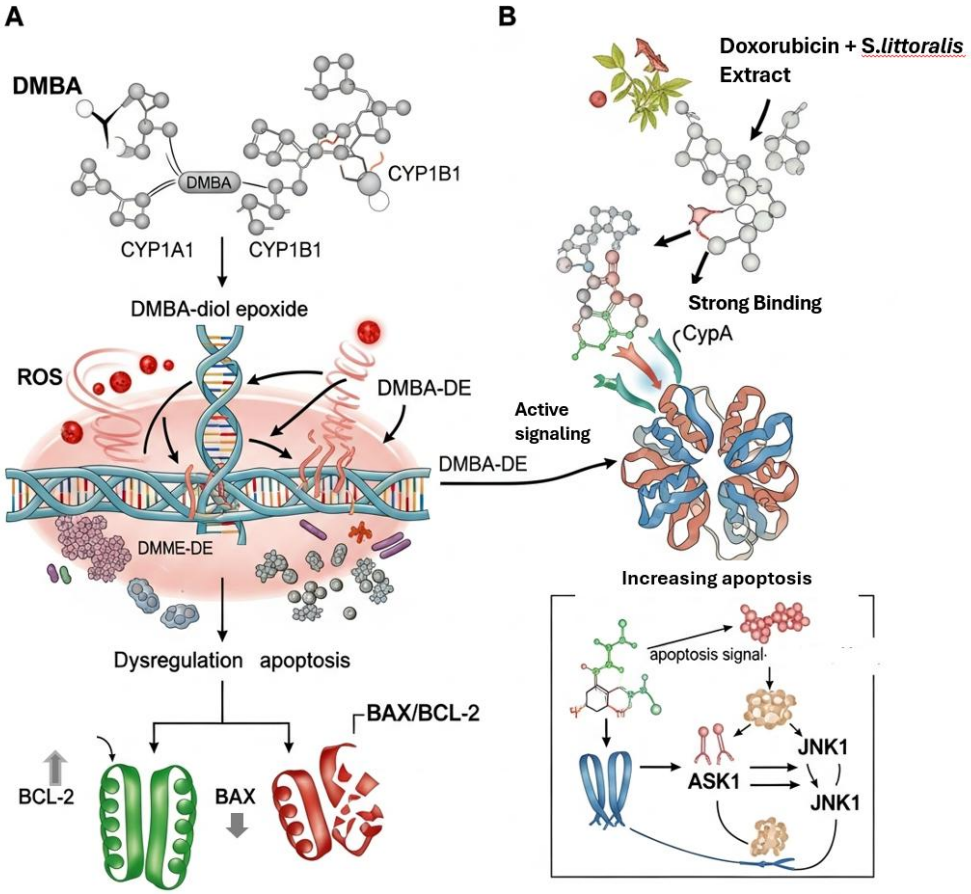

Figure 6 Proposed molecular pathway of anticancer activity in DMBA-induced breast cancer in female sprague-dawley rats. (A) Carcinogenic pathway of 7,12-dimethylbenz[a]anthracene (DMBA). Metabolic activation by cytochrome P450 enzymes (CYP1A1 and CYP1B1) produces DMBA-diol epoxide (DMBA-DE), leading to DNA damage, oxidative stress, dysregulation of apoptosis, and tumor development. (B) Proposed therapeutic pathway of *Spatholobus littoralis* extract in combination with doxorubicin. Bioactive compounds are predicted to target Cyclophilin A (CypA) and activate the ASK1-JNK1 signaling pathway, resulting in BAX upregulation, BCL-2 downregulation, apoptosis induction, and suppression of tumor growth.

DMBA-induced carcinogenesis is initiated through metabolic activation by cytochrome P450 enzymes (CYP1A1/CYP1B1), generating the reactive metabolite DMBA-diol epoxide (DMBA-DE), which forms DNA adducts and triggers oxidative stress. This condition leads to dysregulation of apoptosis, characterized by increased BCL-2 and decreased BAX expression, resulting in a reduced BCL-2/BAX ratio that supports tumor cell survival. Treatment with the S. *littoralis* extract combination with doxorubicin shows potential to counteract these effects. *In silico* analysis demonstrates that active compounds exhibit strong binding affinity toward Cyclophilin A (CypA), with better predicted bioavailability compared to doxorubicin. This interaction is proposed to activate the CypA-ASK1-JNK1 signaling pathway, leading to upregulation of BAX and downregulation of BCL-2, thereby increasing the BCL-2/BAX ratio and promoting apoptosis. These molecular effects are consistent with *in vivo* findings, including reduced tumor volume, increased tumor growth inhibition (%TGI), and stable body weight, indicating effective tumor suppression with low systemic toxicity.

Conclusions

The *in silico* analysis demonstrated that active compound N-2-[4-(3,3-dimethylallyloxy)phenyl]ethy-licnnamide derived from S. *littoralis* exhibit strong binding affinity toward Cyclophilin A (CypA), with better predicted bioavailability compared to

doxorubicin. This suggests that these compounds may effectively interact with upstream molecular targets involved in apoptotic regulation. The downstream effects of this interaction were supported by *in vivo* findings. Treatment resulted in increased expression of the pro-apoptotic marker BAX and decreased expression of the anti-apoptotic marker BCL-2, leading to an elevated BCL-2/BAX ratio. These molecular changes were consistent with the observed reduction in tumor volume and increased tumor growth inhibition (%TGI) in the treatment groups, particularly in the ADJ 3 group. Therefore, this study indicates that the therapeutic effect of the combination of doxorubicin and *S. littoralis* extract is likely mediated through the regulation of apoptotic signaling, resulting in effective tumor suppression while minimizing toxicity. Nevertheless, the study is limited by its reliance on preclinical models and in silico analyses. Additional validation at the protein level, as well as translational studies in more clinically relevant models, are required to strengthen and confirm these findings. Future research may focus on experimental verification of the molecular mechanisms and evaluation of the clinical potential of these compounds.

Acknowledgements

The authors would like to express their great appreciation to the Indonesian Education Scholarship (BPI), the Center for Higher Education Funding and Assessment, and the Indonesia Endowment Fund for Education (LPDP) for their financial support. The authors also acknowledge the Doctoral Program in Biomedical Science, Faculty of Medicine, Universitas Indonesia, for providing facilities that supported the research and the completion of the necessary data.

Declaration of Generative AI in Scientific Writing

The authors acknowledge the use of generative AI tools (QuillBot and ChatGPT) in the preparation of this manuscript, specifically for language editing and grammar correction. No content generation or data interpretation was performed by AI. The authors take full responsibility for the content and conclusions of this work

CRediT Author Statement

Ois Nurcahyanti: Conceptualization, Methodology, Investigation (*in-vivo* experiments), Data Curation, Formal Analysis, Writing-Original Draft, Writing-Review & Editing **Kusmardi kusmardi:** Conceptualization, Methodology, Formal Analysis, Validation, Writing-Review & Editing **Noorwati Sutandyo:** Formal analysis, Investigation. **Aryo Tedjo:** Software, Formal analysis, Investigation, Validation. **Vivian Soetikno:** Resources, Supervision, Conceptualization, Methodology, Data Curation, Writing-Review & Editing. Visualization.

References

[1] H Sung, J Ferlay, RL Siegel, M Laversanne, I Soerjomataram, A Jemal and F Bray. Global cancer statistics 2020: GLOBOCAN estimates of incidence and mortality worldwide for 36 cancers in 185 countries. *CA: A Cancer Journal for Clinicians* 2021; **71(3)**, 209-249.

[2] P Dong and DA Gewirtz. Editorial: Risks and benefits of adjuvants to cancer therapies. *Frontiers in Oncology* 2022; **12**, 10-12.

[3] M Kciuk, A Gielecinska, S Mujwar, D Kolat, Z Kaluzinska-Kolat, I Celik and R Kontek. Doxorubicin - an agent with multiple mechanisms of anticancer activity. *Cells* 2023; **12(4)**, 659.

[4] U Anand, A Dey, AK Singh Chandel, R Sanyal, A Mishra, DK Pandey, V De Falco, A Upadhyay, R Kandimalla, A Chaudhary, JK Dhanjal, S Dewanjee, J Vallamkondu and JMP de la Lastra. Cancer chemotherapy and beyond: Current status, drug candidates, associated risks and progress in targeted therapeutics. *Genes & Diseases* 2023; **10(4)**, 1367-1401.

[5] H Dariushnejad, N Roshanravan, HM Wasman, M Cheraghi, L Pirzeh and V Ghorbanzadeh. Silibinin, synergistically enhances vinblastine-mediated apoptosis in triple negative breast cancer cell line: Involvement of Bcl2/Bax and caspase-3 pathway. *International Journal of Hematology-Oncology and Stem Cell Research* 2024; **18(2)**, 174.

[6] G Pistritto, D Trisciuoglio, C Ceci, A Garufi and G D'Orazi. Apoptosis as anticancer mechanism: Function and dysfunction of its modulators and

targeted therapeutic strategies. *Aging* 2016; **8(4)**, 603-619.

[7] DE Pritchard, S Ceryak, KE Ramsey, TJ O'Brien, L Ha, JL Fornsaglio, DA Stephan and SR Patierno. Resistance to apoptosis, increased growth potential, and altered gene expression in cells that survived genotoxic hexavalent chromium [Cr(VI)] exposure. *Molecular and Cellular Biochemistry* 2005; **279(1-2)**, 169-181.

[8] P Hussar. Apoptosis regulators Bcl-2. *Encyclopedia* 2022; **2(4)**, 1624-1636.

[9] R Singh, A Letai and K Sarosiek. BCL-2 family protein. *Definitions* 2020; **20(3)**, 175-193.

[10] MA O'Brien and R Kirby. Apoptosis: A review of pro-apoptotic and anti-apoptotic pathways and dysregulation in disease. *Journal of Veterinary Emergency and Critical Care* 2008; **18(6)**, 572-585.

[11] J Han, MK Lee, Y Jang, WJ Cho and M Kim. Repurposing of cyclophilin A inhibitors as broad-spectrum antiviral agents. *Drug Discovery Today* 2022; **27(7)**, 1895-1912.

[12] L Liu, L Zuo, J Yang, S Xin, J Zhang, J Zhou, G Li, J Tang and J Lu. Exosomal cyclophilin A as a novel noninvasive biomarker for Epstein-Barr virus associated nasopharyngeal carcinoma. *Cancer Medicine* 2019; **8(6)**, 3142-3151.

[13] S Jin, M Zhang and X Qiao. Cyclophilin A: Promising target in cancer therapy. *Cancer Biology & Therapy* 2024; **25(1)**, 2425127.

[14] WT Stauffer, AZ Goodman and PA Gallay. Cyclophilin inhibition as a strategy for the treatment of human disease. *Frontiers in Pharmacology* 2024; **15**, 1417945.

[15] Y Liao, D Luo, K Peng and Y Zeng. Cyclophilin A: A key player for etiological agent infection. *Applied Microbiology and Biotechnology* 2021; **105(4)**, 1365-1377.

[16] A Abdullah, R Abdullah, Z Nazariah, K Balakrishnan, FJ Abdullah, J Bala and MA Mohd-Lila. Cyclophilin A as a target in the treatment of cytomegalovirus infections. *Antiviral Chemistry and Chemotherapy* 2018; **26**, 2040206618811413.

[17] L Chen, Z Zeng, H Luo, H Xiao and Y Zeng. The effects of CypA on apoptosis: Potential target for the treatment of diseases. *Applied Microbiology and Biotechnology* 2023; **108(1)**, 28.

[18] B Wang, Y Ma, Y Zhang and X Yin. Therapeutic potential of ASK1 activators in cancer treatment: Current insights and future directions. *Biomedicine & Pharmacotherapy* 2024; **178**, 117214.

[19] H Kim, Y Oh, K Kim, S Jeong, S Chon, D Kim, MH Jung, YK Pak, J Ha, I Kang and W Choe. Cyclophilin A regulates JNK/p38-MAPK signaling through its physical interaction with ASK1. *Biochemical and Biophysical Research Communications* 2015; **464(1)**, 112-117.

[20] P. Nigro, G. Pompilio, and M. C. Capogrossi, "Cyclophilin A: A key player for human disease," *Cell Death Dis* 2013;**4(10),** 1–10.

[21] BNA Susanto and N Zayani. The effect of Bajakah (*Spatholobus littoralis* Hassk) stem extract on calculation of leukocyte in mice (*Mus musculus*). *The International Conference on Public Health Proceeding* 2021; **6(1)**, 1100-1106.

[22] DW Rousdy, ERP Wardoyo and S Ifadatin. Anti-inflammatory activity of Bajakah stem (*Spatholobus littoralis* Hassk.) ethanolic extract in carrageenan-induced paw edema mice. *Jurnal Biodjati* 2022; **7(1)**, 66-74.

[23] H Hamzah, SUT Pratiwi, A Jabbar, AS Hafifah, BA Al-Fajri and N Nurhalisah. Bioactivity tracing of the ethanol extract of Bajakah Tampala (*Spatholobus littoralis* Hassk.) typical plant of Kalimantan Island as antibiofilm of *Staphylococcus aureus*. *Open Access Macedonian Journal of Medical Sciences* 2023; **11(A)**, 8-14.

[24] G D'Urso, A Capuano, F Fantasma, MG Chini, V de Felice, G Saviano, G Lauro, A Casapullo, G Bifulco and M Iorizzi. The role of LC-MS in profiling bioactive compounds from plant waste for cosmetic applications: A general overview. *Plants* 2025; **14(15)**, 2284.

[25] KD Oliveira, GU Avanzo, MV Tedardi, MM Rangel, JL Avanzo, H Fukumasu, KVK Rao, IL Sinhorini and MLZ Dagli. Chemical carcinogenesis by DMBA (7,12-dimethylbenzanthracene) in female BALB/c mice: New facts. *Brazilian Journal of Veterinary Research and Animal Science* 2015; **52(2)**, 125-133.

[26] MM Williams and RS Cook. Bcl-2 family proteins in breast development and cancer: Could Mcl-1

targeting overcome therapeutic resistance? *Oncotarget* 2015; **6(6)**, 3519-3530.

[27] H Azimian, M Dayyani, MTB Toossi and M Mahmoudi. Bax/Bcl-2 expression ratio in prediction of response to breast cancer radiotherapy. *Iranian Journal of Basic Medical Sciences* 2018; **21(3)**, 325-332.

[28] S Jin, M Zhang and X Qiao. Cyclophilin A: Promising target in cancer therapy. *Cancer Biology & Therapy* 2024; **25(1)**, 2425127.

[29] K Tabatabaei, S Moazzezi, M Emamgholizadeh, H Vaez, B Baradaran and B Shokouhi. Improved therapeutic efficacy of doxorubicin chemotherapy with cannabidiol in 4T1 mice breast cancer model. *Cancer Medicine* 2024; **13(21)**, e70395.

[30] F Ismed, WN Desti, N Arifa, R Rustini and DP Putra. *TLC-bioautographic and LC-MS/MS detection of antimicrobial compounds from four semipolar extracts of Cladonia species. In*: Zaini (Ed.). Proceedings of the 2nd International Conference on Contemporary Science and Clinical Pharmacy. Atlantis Press, Dordrecht, Netherlands, 2021, p. 49-59.

[31] AE Wibowo, S Sriningsih, PE Wuyung and R Ranasasmita. The influence of DMBA (7,12-dimethylbenz-[a]anthracene) regimen in the development of mammae carcinogenesis on Sprague Dawley female rat. *Indonesian Journal of Cancer Chemoprevention* 2010; **1(1)**, 60-66.

[32] NK Rusdi. 2022, Potensi ekstrak tertarget lunasin pada penghambatan karsinogenesis kanker payudara tikus sprague dawley yang diinduksi DMBA (*in Indonesian*). Ph. D. Dissertation. Universitas Indonesia, Jawa Barat, Indonesia, 2022.

[33] MM Jensen, JT Jorgensen, T Binderup and A Kjaer. Tumor volume in subcutaneous mouse xenografts measured by microCT is more accurate and reproducible than determined by ^{18}F-FDG-microPET or external caliper. *BMC Medical Imaging* 2008; **8**, 16.

[34] BPOM. *Pedoman uji toksisitas pra-klinik secara in vivo* (*in Indonesian*). Badan Pengawas Obat dan Makanan Republik Indonesia, Jakarta, Indonesia, 2022.

[35] MM Tomayko and CP Reynolds. Determination of subcutaneous tumor size in athymic (nude) mice. *Cancer Chemotherapy and Pharmacology* 1989; **24**, 148-154.

[36] JD Sun, Q Liu, J Wang, D Ahluwalia, D Ferraro, Y Wang, JX Duan, WS Ammons, JG Curd, MD Matteucci, CP Hart. Selective tumor hypoxia targeting by hypoxia-activated prodrug TH-302 inhibits tumor growth in preclinical models of cancer. *Clinical Cancer Research* 2012; **18(3)**, 758-770.

[37] H Chen, Q Ye, J Lv, P Ye, Y Sun, S Fan, X Su, P Gavine and X Yin. Evaluation of trastuzumab anti-tumor efficacy and its correlation with HER-2 status in patient-derived gastric adenocarcinoma xenograft models. *Pathology & Oncology Research* 2015; **21(4)**, 947-955.

[38] KJ Livak and TD Schmittgen. Analysis of relative gene expression data using real-time quantitative PCR and the 2-delta-delta CT method. *Methods* 2001; **25(4)**, 402-408.

[39] ARRS Brilhante, GR de Sousa, AKS de Aquino-Vital, NTR de Lima, RBL Souza, TA de Souza, MT Scotti, JMB Filho, JF Tavares and MS da Silva. Fabaceae flavonoids beyond the commonplace: A review of chemical diversity, pharmacological activities, mass spectrometric profiling and in silico insights into their subclasses. *Plants* 2025; **14(23)**, 3549.

[40] W Liu, Y Feng, S Yu, Z Fan, X Li, J Li and H Yin. The flavonoid biosynthesis network in plants. *International Journal of Molecular Sciences* 2021; **22(23)**, 12824.

[41] V Ninkuu, OO Aluko, J Yan, H Zeng, G Liu, J Zhao, H Li, S Chen and FD Dakora. Phenylpropanoids metabolism: Recent insight into stress tolerance and plant development cues. *Frontiers in Plant Science* 2025; **16**, 1571825.

[42] L Xu and X Wang. A comprehensive review of phenolic compounds in horticultural plants. *International Journal of Molecular Sciences* 2025; **26(12)**, 5767.

[43] P Nigro, K Satoh, MR O'Dell, NN Soe, Z Cui, A Mohan, J Abe, JD Alexis, JD Sparks and BC Berk. Cyclophilin A is an inflammatory mediator that promotes atherosclerosis in apolipoprotein E-deficient mice. *Journal of Experimental Medicine* 2011; **208(1)**, 53-66.

[44] C Xue, M Sowden and BC Berk. Extracellular Cyclophilin A, especially acetylated, causes pulmonary hypertension by stimulating endothelial apoptosis, redox stress, and inflammation. *Arteriosclerosis, Thrombosis, and Vascular Biology* 2017; **37(6)**, 1138-1146.

[45] WT Stauffer, AZ Goodman and PA Gallay. Cyclophilin inhibition as a strategy for the treatment of human disease. *Frontiers in Pharmacology* 2024; **15**, 1-15.

[46] CA Lipinski. Lead- and drug-like compounds: The rule-of-five revolution. *Drug Discovery Today: Technologies* 2004; **1(4)**, 337-341.

[47] D Veber, S Johnson, HY Cheng, B Smith, K Ward and K Kopple. Molecular properties that influence the oral bioavailability of drug candidates. *Journal of Medicinal Chemistry* 2002; **45**, 2615-2623.

[48] O Tacar, P Sriamornsak and CR Dass. Doxorubicin: An update on anticancer molecular action, toxicity and novel drug delivery systems. *Journal of Pharmacy and Pharmacology* 2013; **65(2)**, 157-170.

[49] CF Thorn, C Oshiro, S Marsh, T Hernandez-Boussard, H McLeod, TE Klein and RB Altman. Doxorubicin pathways: Pharmacodynamics and adverse effects. *Pharmacogenetics and Genomics* 2011; **21(7)**, 440-446.

[50] A Daina, O Michielin and V Zoete. SwissADME: A free web tool to evaluate pharmacokinetics, drug-likeness and medicinal chemistry friendliness of small molecules. *Scientific Reports* 2017; **7(1)**, 42717.

[51] LE Anderson, JE Morris, LB Sasser and RG Stevens. Effect of constant light on DMBA mammary tumorigenesis in rats. *Cancer Letters* 2000; **148(2)**, 121-126.

[52] BV Asbroeck, DN Kruger, SV den Bogaert, D Dombrecht, M Bosman, EMV Craenenbroeck, PJ Guns and EV Breda. Distinct impact of doxorubicin on skeletal muscle and fat metabolism in mice: Without dexrazoxane effect. *International Journal of Molecular Sciences* 2025; **26(3)**, 1177.

[53] I Mentoor, T Nell, Z Emjedi, PJ van Jaarsveld, L de Jager and AM Engelbrecht. Decreased efficacy of doxorubicin corresponds with modifications in lipid metabolism markers and fatty acid profiles in breast tumors from obese vs. lean mice. *Frontiers in Oncology* 2020; **10**, 306.

[54] J Dickinson, MD Matas, PA Dickinson and HB Mistry. Exploring a model-based analysis of patient derived xenograft studies in oncology drug development. *PeerJ* 2021; **9**, 1-10.

[55] PS Cella, RLN de Matos, PC Marinello, JC da Costa, FA Moura, APAFRL Bracarense, P Chimin and R Deminice. Doxorubicin causes cachexia, sarcopenia, and frailty characteristics in mice. *PLoS One* 2024; **19(4)**, e0301379.

[56] A Elfadadny, RF Ragab, R Hamada, SK Al Jaouni, J Fu, SA Mousa and AH El-Far. Natural bioactive compounds-doxorubicin combinations targeting topoisomerase II-alpha: Anticancer efficacy and safety. *Toxicology and Applied Pharmacology* 2023; **461**, 116405.

[57] D Tungmunnithum, S Drouet, JM Lorenzo and C Hano. Characterization of bioactive phenolics and antioxidant capacity of edible bean extracts of 50 Fabaceae populations grown in Thailand. *Studies in Natural Products Chemistry* 2021; **58(12)**, 389-417.

[58] Z Zhang, L Hou, D Liu, S Luan, M Huang and L Zhao. Directly targeting BAX for drug discovery: Therapeutic opportunities and challenges. *Acta Pharmaceutica Sinica B* 2024; **14(6)**, 2378-2401.

[59] M Kumar, V Kaur, S Kumar and S Kaur. Phytoconstituents as apoptosis inducing agents: Strategy to combat cancer. *Cytotechnology* 2016; **68(4)**, 531-563.

[60] Q Wang, L Zhang, X Yuan, Y Ou, X Zhu, Z Cheng, P Zhang, X Wu, Y Meng and L Zhang. The relationship between the Bcl-2/Bax proteins and the mitochondria-mediated apoptosis pathway in the differentiation of adipose-derived stromal cells into neurons. *PLoS One* 2016; **11(10)**, e0163327.

[61] S Zamorano, D Rojas-Rivera, F Lisbona, V Parra, FA Court, R Villegas, EH Cheng, SJ Korsmeyer, S Lavandero and C Hetz. A BAX/BAK and cyclophilin D-independent intrinsic apoptosis pathway. *PLoS One* 2012; **7(6)**, e37782.

[62] Z Qian, X Zhao, M Jiang, W Jia, C Zhang, Y Wang, B Li and W Yue. Downregulation of cyclophilin A by siRNA diminishes non-small cell

lung cancer cell growth and metastasis via the regulation of matrix metallopeptidase 9. *BMC Cancer* 2012; **12(1)**, 442.

[63] Y Chen, N Li, J Yang, K Li, M Tang, X Zhao, W Guo, A Tong, C Nie, Y Peng and Z Yuan. PUMA overexpression dissociates thioredoxin from ASK1 to activate the JNK/BCL-2/BCL-XL pathway augmenting apoptosis in ovarian cancer. *Biochimica et Biophysica Acta: Molecular Basis of Disease* 2022; **12**, 1868.

[64] S Hafezi and M Rahmani. Targeting BCL-2 in cancer: Advances, challenges, and perspectives. *Cancers* 2021; **13(6)**, 1292.

[65] S Barille-Nion, S Lohard and PP Juin. Targeting of BCL-2 family members during anticancer treatment: A necessary compromise between individual cell and ecosystemic responses? *Biomolecules* 2020; **10(8)**, 1109.